

1-1-2002

# Uniqueness of Bilevel Image Degradations

Elisa H. Barney Smith  
*Boise State University*

## Uniqueness of bilevel image degradations

Elisa H. Barney Smith \*

Electrical and Computer Engineering Department  
Boise State University, Boise, Idaho 83725, USA

### ABSTRACT

Two major degradations, edge displacement and corner erosion, change the appearance of bilevel images. The displacement of an edge determines stroke width, and the erosion of a corner affects crispness. These degradations are functions of the system parameters: the point spread function (PSF) width and functional form, and the binarization threshold. Changing each of these parameters will affect an image differently. A given amount of edge displacement or amount of erosion of black or white corners can be caused by several combinations of the PSF width and the binarization threshold. Any pair of these degradations are unique to a single PSF width and binarization threshold for a given PSF function. Knowledge of all three degradation amounts provides information that will enable us to determine the PSF functional form from the bilevel image. The effect of each degradation on characters will be shown. Also, the uniqueness of the degradation triple  $\{d_w, d_b, \delta_c\}$  and the effect of selecting an incorrect PSF functional form will be shown, first with relation to PSF width and binarization threshold estimate, then for how this is visible in sample characters.

### 1. INTRODUCTION

Bilevel processes, such as scanning, photocopying, faxing, and printing, cause many degradations to document images. These processes are characterized by spatial and intensity quantization, which change the appearance of the image content, such as characters and line drawings. This paper discusses bilevel degradations in the context of the scanning process. If the degradations that are introduced when a document passes through a bilevel process can be characterized, a training set more closely matching the document image can be selected for optical character recognition. This is an important step toward improving recognition accuracy [3].

Figure 1 shows a model of the production of bilevel digitized images through the scanning process. The parameters of this model are the PSF functional form, the PSF width and the binarization threshold. Image degradations are caused by a joint effect of the convolution with the point spread function, and the thresholding. Each combination of PSF and binarization threshold produces a different digitized image. The PSF affects the image by both its functional form,  $PSF()$ , and the width parameter for that function,  $w$ . The PSF form and width will be functions of a scanner manufacturer and any interpolation done while converting from optical resolution. Therefore, documents scanned on different scanners or at different resolutions will usually have different PSF functions and width parameters. The thresholding parameter,  $\Theta$ , is the absorbance level at which the decision on whether a pixel will be black or white is made. This is usually adjustable by either the user or automatically by the scanning software.

PSF shape is not readily available from bilevel images because of the lack of shape information in the edges. Methods for estimating the PSF width,  $w$ , and binarization threshold,  $\Theta$ , have been proposed in [5, 6, 7]. These estimation methods take measurements of the amount of a degradation present in an image and convert this to an estimate of the system parameters  $w$  and  $\Theta$ . To do the estimation requires the PSF functional form to be either known or presumed before estimation could take place. This paper describes how the PSF shape assumption can be verified from measurements of degradations in bilevel images because each degradation combination will be specific to a single PSF form.

This paper starts with an introduction of bilevel image degradation types. It then shows how these affect character images. How these degradations relate to the system parameters is shown next. Comparing the loci of system parameters for sets of degradations shows that the set of three degradations are often unique to a specific PSF form, PSF width and binarization threshold.

### 2. DEGRADATION TYPES

The two most noticeable effects of degradation in a character image are a change in the stroke width and a change in the shape of the corners[8]. The degradation type, more than the scanner system values, is used to describe the image quality.

\* EBarneySmith@boisestate.edu, Phone: 208-426-2214, <http://coen.boisestate.edu/EBarneySmith>

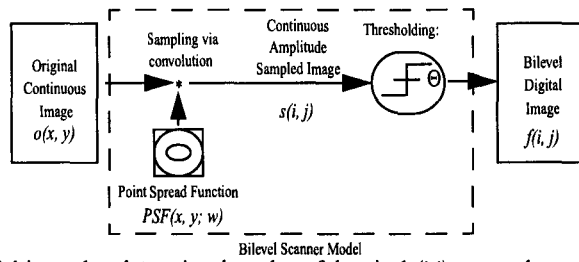


Figure 1: This scanner model is used to determine the value of the pixel  $(i, j)$  centered on each sensor element.

The amount of each degradation can be quantified and related to the PSF function, width and binarization threshold. In the following subsections the degradations will be defined and their relationship to the PSF width and binarization threshold will be shown.

### 2.1 Edge displacement

The stroke width is determined by the location of the edges of the stroke. The stroke width will change as the edge locations move. The distance an edge is displaced depends on the threshold, the PSF width, and the functional form of the PSF. During scanning, an edge separated from other edges by a distance greater than the support of the PSF changes from a step to an edge spread function, ESF, through convolution with the PSF. This is then thresholded to reform a step edge, as shown in Figure 2. The amount an edge was displaced after scanning,  $\delta_c$ , was shown in [4] to be related to  $w$  and  $\Theta$  by

$$\delta_c = -w \text{ESF}^{-1}(\Theta) . \quad (1)$$

An infinite number of  $(w, \Theta)$  values could produce any one  $\delta_c$  value. A threshold  $\Theta < 1/2$  produces a positive edge displacement (stroke widens), while a threshold value greater than  $1/2$  will produce a negative edge displacement (stroke narrows). The curves for  $\delta_c$  and  $-\delta_c$  are symmetric around the  $\Theta = 1/2$  line if the PSF is symmetric. If  $\Theta = 1/2$ , then  $\delta_c = 0$  for all values of  $w$ . Figure 3 shows loci of  $(w, \Theta)$  at 5 different constant  $\delta_c$  values for three PSF functions. They share the symmetry and overall trends but have a shape specific to the PSF functional form.

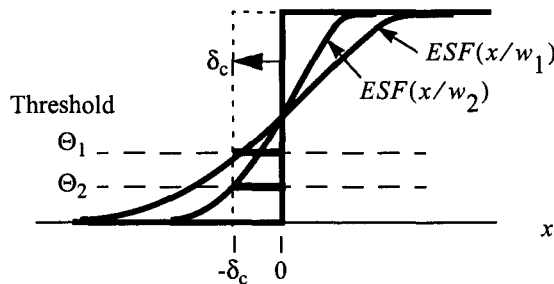


Figure 2: Edge after blurring with a generic PSF at two widths,  $w$ . The two thresholds shown produce the same edge shift  $\delta_c$ .

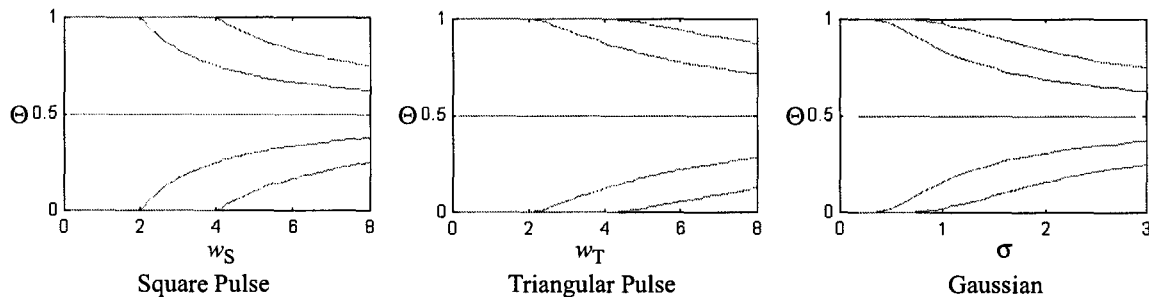


Figure 3: Loci of constant edge spread,  $\delta_c = [-2 -1 0 1 2]$  (from top to bottom) for 3 PSF functions.

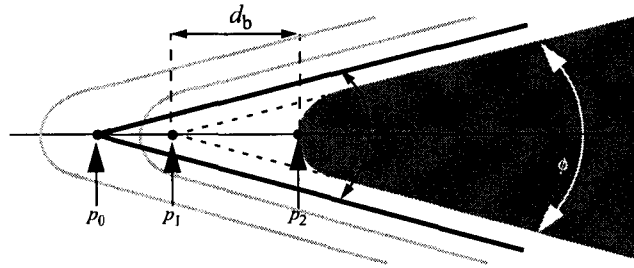


Figure 4: The blurred corner (grey area and lines) may be displaced from the original corner position (black line) in three different ways. The visible erosion,  $d_b$ , is the same for all three.

## 2.2 Corner erosion

The other major degradation important to bilevel images is the shape of a corner after scanning [7]. At a distance greater than one half the support of the PSF from the corner, only edge spread effects described above are present. Nearer to the intersection of the two edges, a degradation is caused by the interaction of the two edges. The degradation of a corner can occur in three forms, shown in Figure 4, depending on the threshold and the angle of the corner. The point  $p_0$  is the apex of the original corner. The point  $p_2$  is the point along the angle bisector of the new rounded corner where the blurred corner equals the threshold value. The point  $p_1$  is the point where the new corner edges would intersect if extrapolated. The distance that a corner appears to be eroded from the displaced edges depends on the threshold, the PSF width, and the PSF functional form. This is shown as the distance  $d_b$  in Figure 4. In [6] and [7], the distance was shown to be

$$d_b = \frac{-wESF^{-1}(\Theta)}{\sin(\phi/2)} + f_b^{-1}(\Theta; w, \phi), \quad (2)$$

where

$$f_b(d_{0b}; w, \phi) = \int_{x=0}^{x=\infty} \int_{y=-x \tan \frac{\phi}{2}}^{y=x \tan \frac{\phi}{2}} PSF(x - d_{0b}, y; w) dy dx. \quad (3)$$

The measurement of the distance the corner is eroded from the original corner,  $\overline{p_0 p_2}$ , requires knowledge of the original location of the corner, which is not easily found on its own and does not describe the degradation seen in the character image. The erosion distance is dependent on the angle of the corner,  $\phi$ . The angle  $\phi$  can be easily measured because the scanned edges will be parallel to the original edges at locations sufficiently far from the corner. Larger angles,  $\phi$ , will show less erosion for the same range of  $w$ . A given amount of corner erosion can also occur for an infinite number of  $(w, \Theta)$  values. Samples of  $(w, \Theta)$  loci for constant  $d_b$  at three corner angle measures  $\phi$  are shown in Figure 5.

A white corner on a black background will also be eroded, but in a manner opposite from the black corners. The amount of erosion has the relationship

$$d_w = \frac{-wESF^{-1}(1-\Theta)}{\sin(\phi/2)} + f_b^{-1}(1-\Theta; w, \phi). \quad (4)$$

The loci for the same amount of erosion on black versus white corners are symmetric to each other about the  $\Theta=1/2$  line, similar to the relationship between  $\delta_c$  and  $-\delta_c$ .

## 3. SAMPLE CHARACTERS

These two types of degradation, edge displacement and corner erosion, are present in various combinations for all scanned characters containing both straight lines and corners. To illustrate how each degradation affects characters, 12-point sans-serif font characters x and z are synthetically blurred. The characters are created at 600dpi "scanning" resolution and are shown at four times their standard size in Figures 6 and 7. These characters are created with  $(w, \Theta)$  values that give constant edge spread or constant corner erosion. As each of these degradations can occur for multiple thresholds, PSF widths, and functional forms, each of these parameters are varied to show their effects.

### 3.1 Edge displacement

The loci of  $(w, \Theta)$  values that lead to edge spread values of  $\delta_c = -2, -1, 0, 1$  and  $2$ , were shown in Figure 3. Two  $(w, \Theta)$

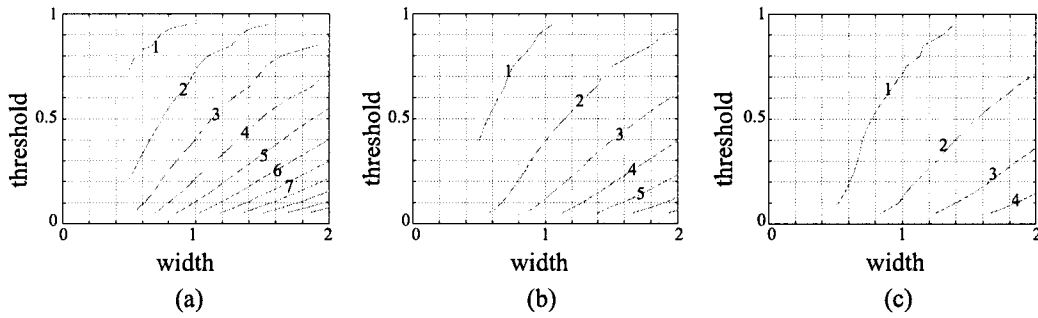


Figure 5: Loci of black corner erosion amounts,  $d_b$ , for a Gaussian PSF (a)  $\phi=\pi/6$  (b)  $\phi=\pi/4$  (c)  $\phi=\pi/3$ .

Edge Displacement	$\delta_c = -2$	$\delta_c = 0$	$\delta_c = 2$
Synthetic Characters	X Z	X Z	X Z
	X Z	X Z	X Z

Figure 6: Comparison of characters with common  $\delta_c$  values produced with two different  $(w, \Theta)$  values using the Gaussian PSF.

values were selected for the Gaussian PSF at each of the  $\delta_c$  values -2, 0 and 2. These values were used to generate synthetic characters shown in Figure 6. The difference in the  $(w, \Theta)$  values is large, but the characters appear quite similar because of the constant  $\delta_c$ . Differences can still be seen among characters with a constant  $\delta_c$ , particularly at image corners. This is because the  $\delta_c$  calculation is only valid when the edges are isolated from other edges.

### 3.2 Corner erosion

For constant corner erosion, the angles present in the characters affect the corner erosion. The locus of  $(w, \Theta)$  points that give constant corner erosion of  $d$  for an angle  $\phi_1$  will not give a constant corner erosion for an angle  $\phi_2$ . Figure 7 shows characters created with  $(w, \Theta)$  values selected from the loci in Figure 5c to give the corner erosion values of  $d_b=1, 2, 3$  on the outermost black corners of the letter x, and corner erosions  $d_w=1, 2, 3$  for the white corners in the letter z. Both these corners have an approximate measure of  $\phi = \pi/3$  radians.

Within the groups of characters with constant corner erosion, some characters' strokes are widened, some are narrowed. This gives the characters a considerable variation in appearance among characters with the same corner erosion, much more than was seen for characters with equal edge spread and varied corner erosion. The feature people notice most easily in a character is the stroke width. When this is constant, characters appear similar. Characters with constant corner erosion do not usually have the same edge displacement, so the characters in Figure 7 with common corner erosion do not appear similar.

	Black Corner Erosion			White Corner Erosion		
	$d_b = 1$	$d_b = 2$	$d_b = 3$	$d_w = 1$	$d_w = 2$	$d_w = 3$
Synthetic Characters	X Z	X Z	X Z	X Z	X Z	X Z
	X Z	X Z	X Z	X Z	X Z	X Z

Figure 7: Comparison of characters with constant  $d_b$  values for the acute black corners on the tips of the letter x and constant  $d_w$  values for the acute white corners on the interiors of the letter z.

#### 4. UNIQUENESS

Characters created with an array of several PSF widths and binarization thresholds are shown in Figure 8 for two different PSF functional forms. The thresholds used for each set of characters are equivalent, and the widths were chosen to make the edge displacement approximately equal in each pair across the two sets. However, corresponding characters are not identical because of differing corner erosion amounts.

The degradation measures  $\delta_c$ ,  $d_b$  and  $d_w$  all depend on the PSF functional form and the values of the PSF width and the binarization threshold. A constant value for each of the three degradation measures can arise from an infinite number of  $(w, \Theta)$  values for each PSF function. For any two of the three degradations, a unique  $(w, \Theta)$  pair exists in each  $PSF()$  space. When  $\Theta=1/2$ , the edge displacement  $\delta_c=0$  and the black and white corner erosions will be equal,  $d_w=d_b$ . This combination of degradations will occur for all PSF functional forms. When  $\delta_c \neq 0$ , all three loci will intersect at a unique point only when the loci are drawn in the proper PSF space. Here for a given degradation set,  $\{d_w, d_b, \delta_c\}$ , a unique  $\{w, \Theta, PSF()\}$  set exists. Characters made with different PSF will have the same degradation triple  $\{d_w, d_b, \delta_c\}$  only when low resolution makes a change immeasurable. When the edge spread  $\delta_c \neq 0$ , the degradation triple  $\{d_w, d_b, \delta_c\}$  is unique to the PSF functional form, PSF width and binarization threshold and can be used to validate the PSF assumption used in estimating  $w$  and  $\Theta$  in [5, 6, 7].

Figure 9 shows the loci of  $(w, \Theta)$  points for a degradation triple  $\{d_w, d_b, \delta_c\}=\{2, 1, -0.77\}$  for both the bivariate Gaussian PSF and the square pillbox PSF. The  $d_w$  and  $d_b$  loci are drawn for  $\phi=\pi/3$ . These three loci intersect at the point  $(w, \Theta)=(1, 0.78)$  for the Gaussian PSF. For the square PSF, the three lines do not intersect at a single  $(w, \Theta)$  point, nor will they intersect at a single point of other PSF. A similar result will appear for other degradation triples including sets of three  $d_w$  or  $d_b$  from corners of different angles,  $\phi$ . These loci for sets of three  $d_w$  or  $d_b$  will intersect at smaller angles, so the effect of a small error in estimating the degradation amount will have a greater effect on the  $(w, \Theta)$  estimates.

The amount the loci intersection points deviate from a single intersection point depends on the binarization threshold and the difference in the heaviness of the tail in the two PSFs. Systems with a binarization threshold further from  $\Theta=0.5$  will have a larger divergence in intersection points. The tail heaviness can be characterized by the *kurtosis factor* of the PSF. The kurtosis factor is the ratio of the kurtosis to the variance squared

$$kf = \frac{E\{(x-\mu)^4\}}{E\{(x-\mu)^2\}^2} \quad (5)$$

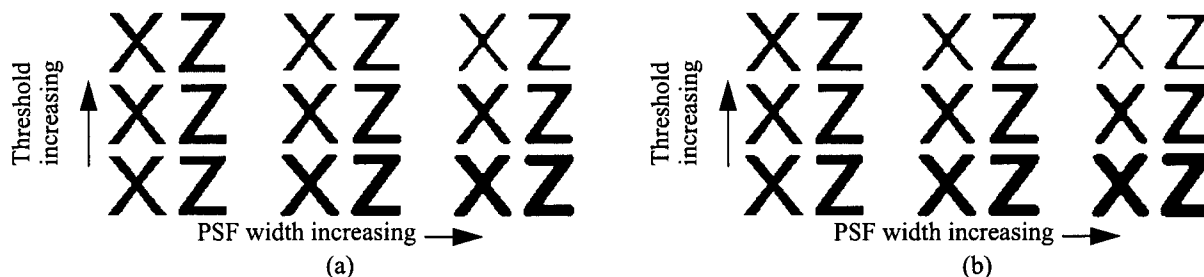


Figure 8: Characters degraded by a range of thresholds and PSF widths for (a) triangular and (b) Gaussian PSF.

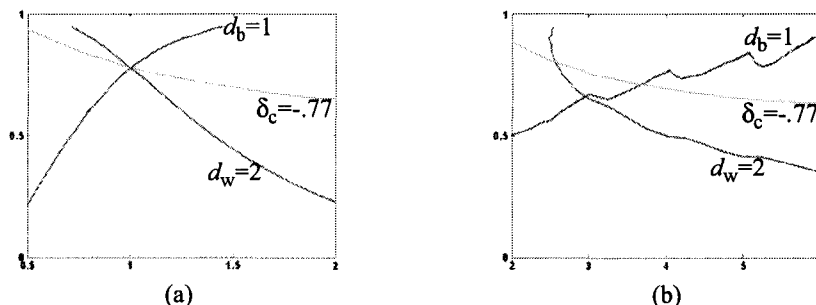


Figure 9: Loci  $d_w=2, d_b=1, \delta_c=-.77$  (a) Gaussian PSF, (b) Square PSF.

Table 1: Kurtosis Factors

PSF Function	Kurtosis Factor
Square Pulse	1.8
Triangular Pulse	2.4
Gaussian	3
Cauchy	undefined, but large

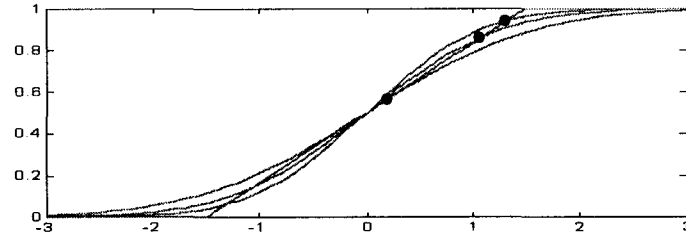


Figure 10: Edge spread functions for square and three Gaussian PSFs. As the threshold changes, the width of the Gaussian PSF needed to intersect the ESF of the square PSF changes.

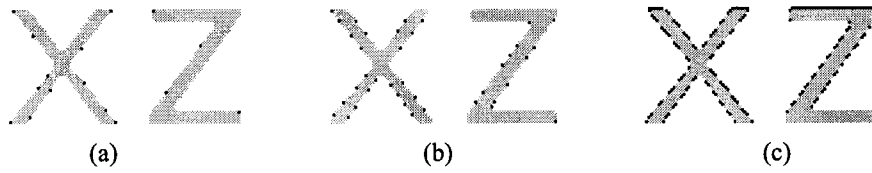


Figure 11: Difference between characters at Gaussian loci 3-way intersection, and square pair wise loci intersections. (a)  $d_w$ ,  $\delta_c$ ; (b)  $d_b$ ,  $\delta_c$ ; (c)  $d_w$ ,  $d_b$ .

For many PSF functional forms the kurtosis factor is a constant, independent of the width parameter. Kurtosis factors for several PSF forms are shown in Table 1. The PSF width needed to give the same effective edge displacement as a PSF of a different form changes as the value of  $\Theta$  changes. This is shown graphically in Figure 10. This difference in functional form manifests itself in the different shape of the  $\delta_c$ ,  $d_b$  and  $d_w$  loci. This was shown in Figure 3 for  $\delta_c$ . A similar change in loci shape occurs for  $d_b$  and  $d_w$ .

Characters were generated using the Gaussian PSF at the three-way ( $w$ ,  $\Theta$ ) intersection point, and using the square PSF at each of the three pair-wise intersection points. The characters  $x$  and  $z$  were selected because the black corner of the  $x$  and the white corner of the  $z$  both measure approximately  $\pi/3$  radians to correspond with the  $\phi$  used in generating the  $d_b$  and  $d_w$  loci in Figure 9. Figure 11 shows the difference between the characters generated with the Gaussian PSF and each of the characters generated with the square PSF. Dark pixels indicate these differences. The first pair of characters have a mismatch in the  $d_b$  degradation (0.5 vs. 1). The tips of the  $x$  show this most clearly. The lack of agreement in the  $d_w$  degradation (2.6 vs. 2) is seen best in the interior corners of the  $z$  in the second set of characters. The third pair of characters show the mismatch in  $\delta_c$  (-0.45 vs. -0.77), which can be seen in the difference in stroke widths. Even though the difference in degradation amounts are each less than one pixel, a difference in the characters can be seen.

The uniqueness of the three-way intersection of degradation loci implies that if the degradation triple  $\{d_w, d_b, \delta_c\}$  can be accurately measured, the binarization threshold, and the PSF form and width parameter can be identified. This provides a method to determine the PSF shape from a bilevel image.

## 5. DISCUSSION

Two bilevel image degradations were introduced: edge displacement,  $\delta_c$ , and corner erosion,  $d_b$  and  $d_w$ . These were related to the bilevel system variables PSF width,  $w$ , and binarization threshold,  $\Theta$ . Each of these degradations can be caused by an infinite number of  $w$  and  $\Theta$  values. Any particular combination of degradations will be unique to a PSF func-

tion and values of PSF width and binarization threshold.

These degradations affect how a character looks after scanning. A larger number of pixels are affected by a change in  $\delta_c$  as compared to the same size change in  $d_b$  or  $d_w$ . This causes characters with a constant edge displacement to have a similar look, even if they were created with different  $w$  and  $\Theta$  values. The change in  $d_b$  or  $d_w$  is harder to see, both because it often relies on the value of a single pixel at the tip of the rounded corner and because we base our view of a character's appearance more on the stroke width than the corner rounding.

These two degradation parameters have distinctly different characteristics in how they affect an image. If all three of these parameters can be accurately estimated for a bilevel image, the PSF width, the binarization threshold and the PSF functional form could be found.

## 6. ACKNOWLEDGEMENT

I would like to thank George Nagy for his useful ideas and comments that encouraged this work.

## 7. REFERENCES

1. Henry S. Baird, "Document Image Defect Models," *Proc. IAPR Workshop on Syntactic and Structural Pattern Recognition*, Murry Hill, NJ, June 1990, pp. 13-15. Reprinted in H. S. Baird, H. Bunke, and K. Yamamoto (Eds.), *Structured Document Image Analysis*, Springer Verlag: New York, 1992, pp. 546-556.
2. Henry S. Baird, "Calibration of document image defect models," *Proc. of Second Annual Symposium on Document Analysis and Information Retrieval*, Las Vegas, Nevada, April 1993, pp. 1-16.
3. Henry S. Baird and George Nagy, "A self-correcting 100-font classifier," *Proc. SPIE Document Recognition*, Vol. 2181, San Jose, CA, 9-10 February 1994, pp. 106-115.
4. Elisa H. Barney Smith, "Characterization of Image Degradation Caused by Scanning," *Pattern Recognition Letters*, Vol. 19, No. 13, 1998, pp. 1191-1197.
5. Elisa H. Barney Smith, "Scanner Parameter Estimation Using Bilevel Scans of Star Charts," *Proc. International Conference on Document Analysis and Recognition 2001*, Seattle, WA, 10-13 September 2001, pp. 1164-1168.
6. Elisa H. Barney Smith, *Optical Scanner Characterization Methods Using Bilevel Scans*, Doctoral Thesis, Rensselaer Polytechnic Institute, December, 1998.
7. Elisa H. Barney Smith, "Estimating Scanning Characteristics from Corners in Bilevel Images," *Proc. SPIE Document Recognition and Retrieval VIII*, Vol. 4307, San Jose, CA, 21-26 January 2001, pp.176-183.
8. Elisa H. Barney Smith, "Bilevel Image Degradations: Effects and Estimation," *Proc. 2001 Symposium on Document Image Understanding Technology*, Columbia, MD, 23-25 April 2001, pp. 49-55.
9. Tin Kam Ho and Henry S. Baird, "Large-Scale Simulation Studies in Image Pattern Recognition," *IEEE Transactions on Pattern Analysis and Machine Intelligence*, Vol. 19, No. 10, October 1997, pp. 1067-1079.